

This is an Open Access document downloaded from ORCA, Cardiff University's institutional repository: <https://orca.cardiff.ac.uk/id/eprint/139868/>

This is the author's version of a work that was submitted to / accepted for publication.

Citation for final published version:

Li, Zhibo , Shutts, Samuel , Xue, Ying, Luo, Wei, Lau, Kei May and Smowton, Peter M. 2021. Optical gain and absorption of 1.55 μm InAs quantum dash lasers on silicon substrate. Applied Physics Letters 118 , 131101. 10.1063/5.0043815

Publishers page: <https://doi.org/10.1063/5.0043815>

Please note:

Changes made as a result of publishing processes such as copy-editing, formatting and page numbers may not be reflected in this version. For the definitive version of this publication, please refer to the published source. You are advised to consult the publisher's version if you wish to cite this paper.

This version is being made available in accordance with publisher policies. See <http://orca.cf.ac.uk/policies.html> for usage policies. Copyright and moral rights for publications made available in ORCA are retained by the copyright holders.



Optical gain and absorption of 1.55 μm InAs quantum dash lasers on silicon substrate

Zhibo Li¹, Samuel Shutts¹, Ying Xue², Wei Luo², Kei May Lau², Peter M. Smowton^{1, a)}

AFFILIATIONS

¹EPSRC Compound Semiconductor Manufacturing Hub, School of Physics and Astronomy, Cardiff University, Cardiff, CF24 3AA United Kingdom

²Department of Electronic and Computer Engineering, Hong Kong University of Science and Technology, Hong Kong

a) Author to whom correspondence should be addressed: smowtonpm@cardiff.ac.uk

ABSTRACT

This letter reports on the temperature dependent optical gain and absorption features, including the quantum confined Stark effect, of an InAs/InGaAs quantum-dash laser directly grown on a (001) Si substrate, with the lasing wavelength within the 1.5 - 1.6 μm range. The maximum optical net gain was 22 cm^{-1} and the internal optical loss was $\sim -17 \text{ cm}^{-1}$ at 20 °C. Measurements as a function of injection level indicate that while the required current densities are still high, the intrinsic performance is significantly better than similarly operated InAs quantum dots operating at 1.3 μm and further efforts on growth could be made to reduce the internal optical losses and non-radiative current density. Optical modal absorption spectra were measured as a function of reverse bias from 0 V to 6 V, and a 40 nm redshift was observed in the absorption edge due to the quantum confined Stark effect suggesting potential applications of these material in electro-absorption modulators grown on silicon.

Published under license by AIP Publishing. <https://doi.org/xx.xxxx/x.xxxxxxx>

Employing quantum dot (QD) and/or quantum dash (QDash) based active regions is considered a promising approach for the realization of III-V laser structures directly grown on (001) silicon (Si) substrates. This is primarily because of the tolerance to material defects afforded by carrier localization. For monolithic integration of these lasers with other components, the relative insensitivity to operating temperature and optical feedback and the broad optical gain bandwidth provide further advantages. Over the past few years, considerable progress has been made to achieve epitaxial growth of 1.3 μm QD lasers directly grown on Si, with in-depth research into optical properties and device

reliability.¹⁻⁴ These lasers comprise of InAs QDs incorporated into layers of GaAs-based alloys which have $\sim 4\%$ lattice mismatch to Si. It is highly desirable to access the 1.55 μm lasing wavelength range to meet growing demands in silicon-photonics for long-haul optical communication and sensing technologies. The essential requirement to realize such a QD laser is to achieve high-quality growth of InAs QD active regions with the overall laser structure, utilizing InP-based materials. However, a larger lattice mismatch exists between InP-based materials and Si ($\sim 8\%$), thus inevitably introducing more defects and causing degradation in device performance. Only recently, 1.55 μm Si-based QDash lasers driven by

constant currents have been reported.⁵ These lasers have high operating currents and in this paper we assess the reasons for this and, by characterizing the underlying optical properties, the potential for further significant improvement in laser performance.

We have used Si-based 1.55 μm InAs QDash laser material the same as published in Ref. 5 for this investigation. Broad-area edge-emitting segmented-contact devices are used to study the temperature dependent optical properties, including direct measurements of gain-current characteristics and optical absorption using the variable stripe-length method,⁶ from 20 °C to 80 °C. We also explore the change in absorption characteristics of the structure with temperature, while inducing the quantum confined Stark effect (QCSE) under a range of reverse bias conditions, to understand the potential of the material for other integrated photonic functions.

The Si-based 1.55 μm InAs QDash laser structure was grown by metal organic chemical vapor deposition (MOCVD). The (001) silicon substrate was fully patterned with V-shaped nanogrooves, which have been proven to effectively inhibit anti-phase domains when growing polar molecules (e.g. III-V materials) on non-polar surfaces (e.g. silicon).^{7,8} As represented in Fig 1 (a) a GaAs intermediate layer was grown on such a v-grooved silicon substrate, followed by the InP buffer layer with three periods of strained-layer superlattice (SLS), which act as dislocation filters^{9,10} to further reduce threading dislocations created at the GaAs to InP boundary. The active region consisted of three dash-in-well (DWELL) layers, where each was formed by self-assembled InAs dashes on the InGaAs strained quantum well. A 30 nm InAlGaAs barrier separated each DWELL layer. The rest of the waveguide was formed by 200 nm un-doped InAlGaAs separate-confinement heterostructure (SCH) layers and sandwiched by the InP cladding layers. P-type InGaAs was deposited as the top contact layer. Details of the growth techniques and epi-structure can be found in the recent work.¹¹

To fabricate segmented-contact devices, 100 μm wide broad-area mesas, etched down to the lower InP contact layer were metallized with 50 μm wide, 300 μm pitch segmented Ti/Au p-contacts on top of each mesa and AuGe/Ni/Au n-contacts beside the mesas. A Schema of the segmented-contact structures is given in Fig 1 (b). During measurement, the devices were driven by a

pulsed current source, with 1 μs pulse duration and 5 kHz repetition frequency, to avoid self-heating.

FIG.1. (a) upper: schema of layer stack. (b) lower: schema of segmented contact structure showing sections used and direction of light collection. Absorption spectra are obtained by taking the ratio of the emission spectra when pumping L2 or L1 and Gain by taking the ratio of emission spectra when pumping both L1 and L2 and L1 alone as per reference 6.

Fig.2 (a) gives an example of optical net gain (solid-line) and optical absorption (dash-line) spectra measured at 20 °C with the injection current per segment of 240 mA (red) and 120 mA (blue) respectively. At the long-wavelength range all spectra converge to the value of α_0 of $17 \pm 3 \text{ cm}^{-1}$. This value, while better than previous work,¹² is significantly higher than the typical values for the shorter wavelength InAs dot structures grown at a GaAs lattice constant and will have a significant impact on the threshold current density that can be achieved. While the gain spectra of Fig.2 (a) are useful when plotted as a function of current, they depend upon the quantity of non-radiative recombination much of which may be associated with extrinsic factors such as defect density, which could be improved in the future. Therefore, to better understand the underlying intrinsic performance we make use of the difference between the transparency point (TP), which is indicated in the graph, and the transition energy, as a measure of the degree of population inversion.¹³ The TP is related to the quasi-Fermi level separation (ΔE_i), which must exceed the photon transition energy ($h\nu$) to achieve positive gain.¹⁴ Similar to GaAs based QDs where we have previously used this measure, it is impossible to identify a single transition energy in the QDash spectrum because of the overlap of ensemble energy states, which is a consequence of size fluctuations. Therefore, as a reference, we choose half of the magnitude of the ground state absorption edge (AE) as the measure of transition energy. This choice is self-consistent when comparing results from the same structures at different temperatures and we comment on its consequence when comparing data from different structures later. Before examining the intrinsic performance, we consider the net gain spectra plotted as a function of current density at 20 °C in Fig.2 (b), where the device area is determined from its measured length and the width derived from the near-field profile, which

takes account of current spreading. This QDash material gain and absorption spectra are broad without obvious features that can be attributed to particular quantum confined states. Such highly broadened spectra and large optical loss are reminiscent of early work on InAs/InGaAs QDs¹⁵ when threshold current densities were still a factor of 100 higher than today's optimized structures, e.g. Ref 16. As is the case for the shorter wavelength QDs, broad gain spectra with positive gain over more than 125nm are obtained.

Fig.3 (a) shows the plot of peak net gain obtained from the maximum of each spectrum in Fig 2 (b) and similar data recorded at additional temperatures as a function of current density measured

FIG.2. (a) Net gain (solid-line) and absorption (dash-line) spectra measured at the pumping current of 240 mA and 120 mA per section at 20 °C using segmented contact method. The absorbing section is at 0V. The positions of transparency point (TP) and absorption edge (AE) are also indicated, (b) Detailed net gain spectra as a function of applied current density at 20 °C.

from 20 °C to 80 °C. At one fixed temperature, optical net gain increases with increasing injection current density. At relatively low pumping levels (e.g. 0.33~1.0 kA/cm², 20 °C), there is a rapid increment in the net gain (from -8.5 cm⁻¹ to 10.5 cm⁻¹), whereas at high current density the net gain magnitude increases more slowly. At higher temperatures, the gain magnitude is lower at the same current density. For example, the highest net gain is 22.2 cm⁻¹ under an injection level of 1.67 kA/cm² at 20 °C, but this peak gain magnitude drops to 9.4 cm⁻¹ and to 0.2 cm⁻¹ when the temperature increases to 50 °C and to 80 °C respectively. The current densities required to achieve positive net gain at all temperatures are very high, as might be expected from laser results,⁵ and we now consider whether this is due to extrinsic or intrinsic factors.

The peak net gain is plotted as a function of injection level (TP-AE) in Fig.3 (b). This removes extrinsic factors such as non-radiative recombination. The net gain is negative at low injection level (TP-AE) because the modal gain has not overcome the relatively high internal optical loss. The positive net-gain which contributes to lasing appears with further increase the injection level. However, to maintain a same net gain, it requires a higher level of injection at higher temperatures. This effect has been explained for InAs QD material previously and is attributed to the increased thermal

distribution of carriers among the available energy states, leading to a lower population at any one energy.¹⁴

FIG.3. Temperature-dependent characteristics of (a) peak net gain versus current density, 20 °C to 80 °C, (b) peak net gain versus injection level which is the difference between transparency energy and transition energy, at 20 °C, 50 °C and 80 °C.

Fig.4 shows a comparison of peak modal gain as a function of injection level between InAs QDs grown in GaAs-based material and this work which is InAs QDash grown in InP-based material using the same definitions of TP-AE and under very similar operating conditions. Here, the definition of AE can introduce a rigid shift between the relative x-axis positions of the two datasets. It is clear that the magnitude of gain and differential gain that can be obtained from the QDash material is significantly larger and that the intrinsic performance of the InAs QDash material grown on InP is superior to that of the more developed InAs on GaAs QDs, in this respect. It is highly likely that the significantly higher threshold current densities observed for the former materials are due to extrinsic factors such as defect density. Significant further improvement on reducing these extrinsic factors is required and, as the data of Fig. 4 shows, very worthwhile.

FIG.4. Peak modal gain versus the injection level ($|TP-AE|$) of InAs QDash grown on InP material system and InAs QDs grown on GaAs material system.

To provide an initial assessment of the suitability of these QDash materials grown on Si for modulators, utilizing the electro-absorption effect we measure the evolution of the modal absorption spectra as a function of reverse bias. The voltage was applied to the first (absorbing) section of the segmented contact device with ASE spectra measured from the second section. Fig.5 (a) shows absorption spectra measured at 20 °C with the reversed voltage varied from 0 V to 6 V. A clear red-shift in the absorption edge (AE) can be observed due to the QCSE which had been demonstrated in quantum well and QD structures already.^{17,18} The potential of external electrical field was assumed to be dropped on the un-doped area comprising of the active region and SCH layers,

which has a total thickness of ~ 460 nm. For this InAs QDash grown on InP-based materials, the AE was shifted to lower energy by ~ 19 meV, corresponding to a 40 nm red-shift from 1595 nm to 1635 nm, with the external electrical field increased from 0 kV/cm to 130 kV/cm (external reversed voltage was from 0 V to 6 V) at 20 °C. Compared to the InAs QDs grown on GaAs-based materials, an 8 V external reversed bias caused a 30 meV shift in the ground-state transition energy.¹⁹ However, for the same amount of external electrical field applied (e.g. 130 kV/cm), the transition energy shift was estimated to be ~ 13.6 meV for InAs QDs grown on GaAs-based materials, less than that of the 1.55 μ m InAs QDash grown on InP-based materials.

The extinction ratio (ER), which is obtained by measuring the change in the absorption magnitude from 0-6 V as a function of wavelength from 20 °C to 80 °C is represented in units of dB/mm in Fig.5 (b). The maxima of ER at 20 °C is ~ 4.5 at 1615 nm, and it slightly increased to 4.7 with the corresponding wavelength shifted to 1660 nm at 80 °C. While these results are significantly less advanced than state of the art materials e.g. Ge on Si modulators²⁰, these initial results can be used to explore the possibilities of EAMs based on this material system, and to optimize the modulator design for e.g. the monolithic integration with laser sources.

In summary, we have demonstrated the temperature dependent optical gain and absorption characteristics, and QCSE of Si-based 1.55 μ m InAs QDash laser through segmented contact methods. We conclude that the performance of lasers is still limited at this point. This primarily arises from a high internal optical mode loss and extrinsic non-radiative recombination, both of which may be related to a high remaining defect density. By plotting gain versus injection level, we see that the intrinsic performance is better than more developed InAs on GaAs QD lasers and that further efforts to improve design and growth are very worthwhile. We note that the electro-absorption effect can be used in these materials to produce a basic modulator grown on silicon operating at 1.55 μ m.

This work is supported by the UK Engineering Physical Sciences Research Council (EPSRC) under grant number EP/P006973/1.

Work at HKUST was supported in part by the Research Grants Council of Hong Kong (16212115, 16245216) and the Innovation and Technology Fund (ITS/273/16FP). The data underpinning the results presented in this paper can be found in the Cardiff University data catalogue with the Digital Object Identifier 10.17035/d.2021.0126100515.

FIG.5, (a) modal absorption spectra under a reversed bias of 0 V to 6 V measured at 20 °C, the arrow indicating the redshift with increasing the voltage, (b) the calculated ER from 20 °C to 80 °C.

REFERENCE

- ¹T. Wang, H. Liu, A. Lee, F. Pozzi, and A. Seeds, *Opt. Express* **19** (12), 11381 (2011).
- ²A. Y. Liu, C. Zhang, J. Norman, A. Snyder, D. Lubyshev, J. M. Fastenau, A. W. K. Liu, A. C. Gossard, and J. E. Bowers, *Applied Physics Letters* **104** (4), 041104 (2014).
- ³S. Chen, W. Li, J. Wu, Q. Jiang, M. Tang, S. Shutts, S. N. Elliott, A. Sobiesierski, A. J. Seeds, I. Ross, P. M. Smowton, and H. Liu, *Nature Photonics* **10** (5), 307 (2016).
- ⁴S. Shutts, C. P. Allford, C. Spinnler, Z. Li, A. Sobiesierski, M. Tang, H. Liu, and P. M. Smowton, *IEEE Journal of Selected Topics in Quantum Electronics* **25** (6), 1 (2019).
- ⁵Y. Xue, W. Luo, S. Zhu, L. Lin, B. Shi, and K. M. Lau, *Opt. Express* **28** (12), 18172 (2020).
- ⁶P. Blood, G. M. Lewis, P. M. Smowton, H. Summers, J. Thomson, and J. Lutti, *IEEE Journal of Selected Topics in Quantum Electronics* **9** (5), 1275 (2003).
- ⁷J. Z. Li, J. Bai, C. Major, M. Carroll, A. Lochtefeld, and Z. Shellenbarger, *Journal of Applied Physics* **103** (10), 106102 (2008).
- ⁸Q. Li, K. W. Ng, and K. M. Lau, *Applied Physics Letters* **106** (7), 072105 (2015).
- ⁹N. El-Masry, J. C. L. Tarn, T. P. Humphreys, N. Hamaguchi, N. H. Karam, and S. M. Bedair, *Applied Physics Letters* **51** (20), 1608 (1987).
- ¹⁰M. Tang, S. Chen, J. Wu, Q. Jiang, V. G. Dorogan, M. Benamara, Y. I. Mazur, G. J. Salamo, A. Seeds, and H. Liu, *Opt. Express* **22** (10), 11528 (2014).

This is the author's peer reviewed, accepted manuscript. However, the online version of record will be different from this version once it has been copyedited and typeset.

PLEASE CITE THIS ARTICLE AS DOI: 10.1063/5.0043815

¹¹W. Luo, Y. Xue, J. Huang, L. Lin, B. Shi, and K. M. Lau, *Photon. Res.* **8** (12), 1888 (2020).

¹²S. Zhu, B. Shi, Q. Li, and K. M. Lau, *Applied Physics Letters* **113** (22), 221103 (2018).

¹³M. G. A. Bernard and G. Duraffourg, *physica status solidi (b)* **1** (7), 699 (1961).

¹⁴P. M. Smowton, I. C. Sandall, D. J. Mowbray, H. Y. Liu, and M. Hopkinson, *IEEE Journal of Selected Topics in Quantum Electronics* **13** (5), 1261 (2007).

¹⁵P. M. Smowton, E. Herrmann, Y. Ning, H. D. Summers, P. Blood, and M. Hopkinson, *Applied Physics Letters* **78** (18), 2629 (2001).

¹⁶P. M. Smowton, A. George, I. C. Sandall, M. Hopkinson, and H. Liu, *IEEE Journal of Selected Topics in Quantum Electronics* **14** (4), 1162 (2008).

¹⁷D. A. B. Miller, D. S. Chemla, T. C. Damen, A. C. Gossard, W. Wiegmann, T. H. Wood, and C. A. Burrus, *Physical Review Letters* **53** (22), 2173 (1984).

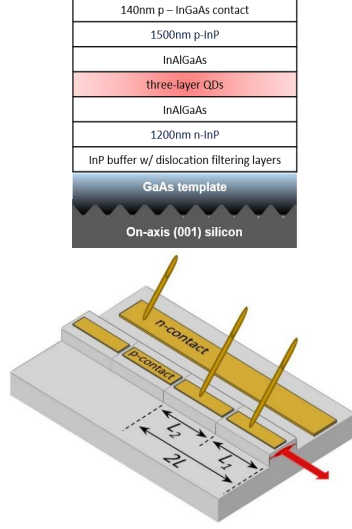
¹⁸H. Xiaodong, A. Stintz, L. Hua, A. Rice, G. T. Liu, L. P. Lester, J. Cheng, and M. J. Malloy, *IEEE Journal of Quantum Electronics* **37** (3), 414 (2001).

¹⁹P. W. Fry, I. E. Itskevich, S. R. Parnell, J. J. Finley, L. R. Wilson, K. L. Schumacher, D. J. Mowbray, M. S. Skolnick, M. Al-Khafaji, A. G. Cullis, M. Hopkinson, J. C. Clark, and G. Hill, *Physical Review B* **62** (24), 16784 (2000).

²⁰S. A. Srinivasan, M. Pantouvaki, S. Gupta, H. T. Chen, P. Verheyen, G. Lepage, G. Roelkens, K. Saraswat, D. Van Thourhout, P. Absil, and J. Van Campenhout, *Journal of Lightwave Technology*, **34**, (2), 419 (2016)

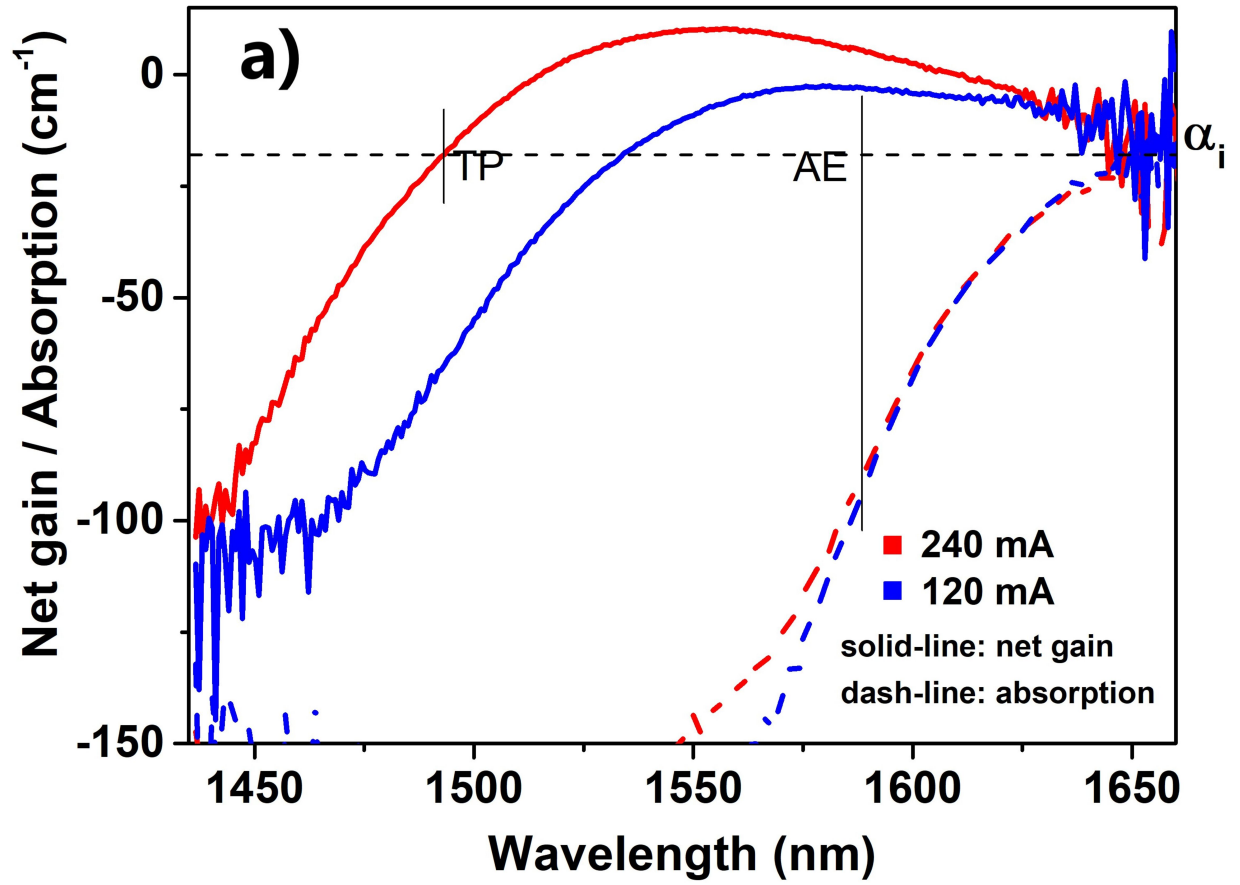
This is the author's peer reviewed, accepted manuscript. However, the online version of record will be different from this version once it has been copyedited and typeset.

PLEASE CITE THIS ARTICLE AS DOI: 10.1063/5.0043815



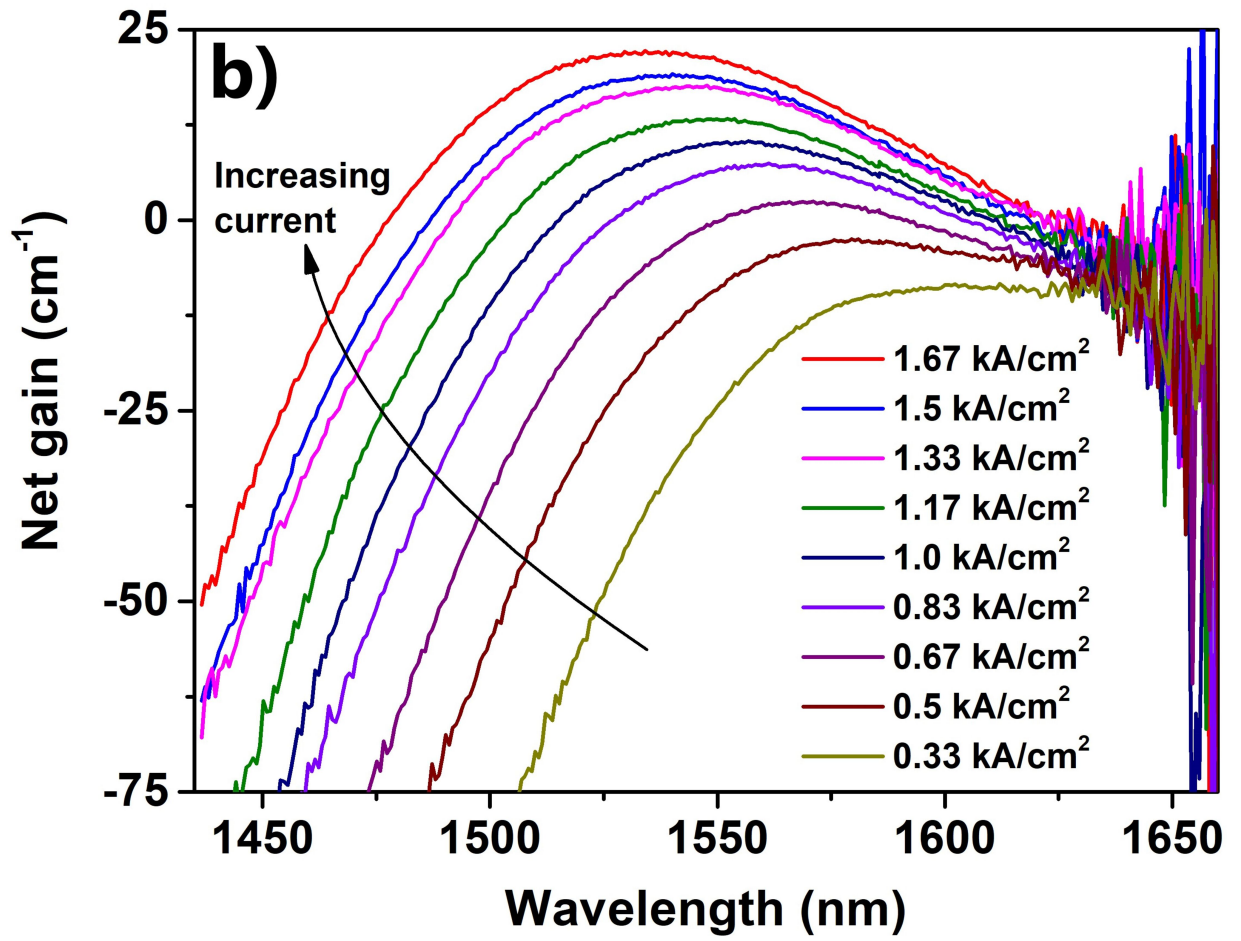
This is the author's peer reviewed, accepted manuscript. However, the online version of record will be different from this version once it has been copyedited and typeset.

PLEASE CITE THIS ARTICLE AS DOI: 10.1063/5.0043815



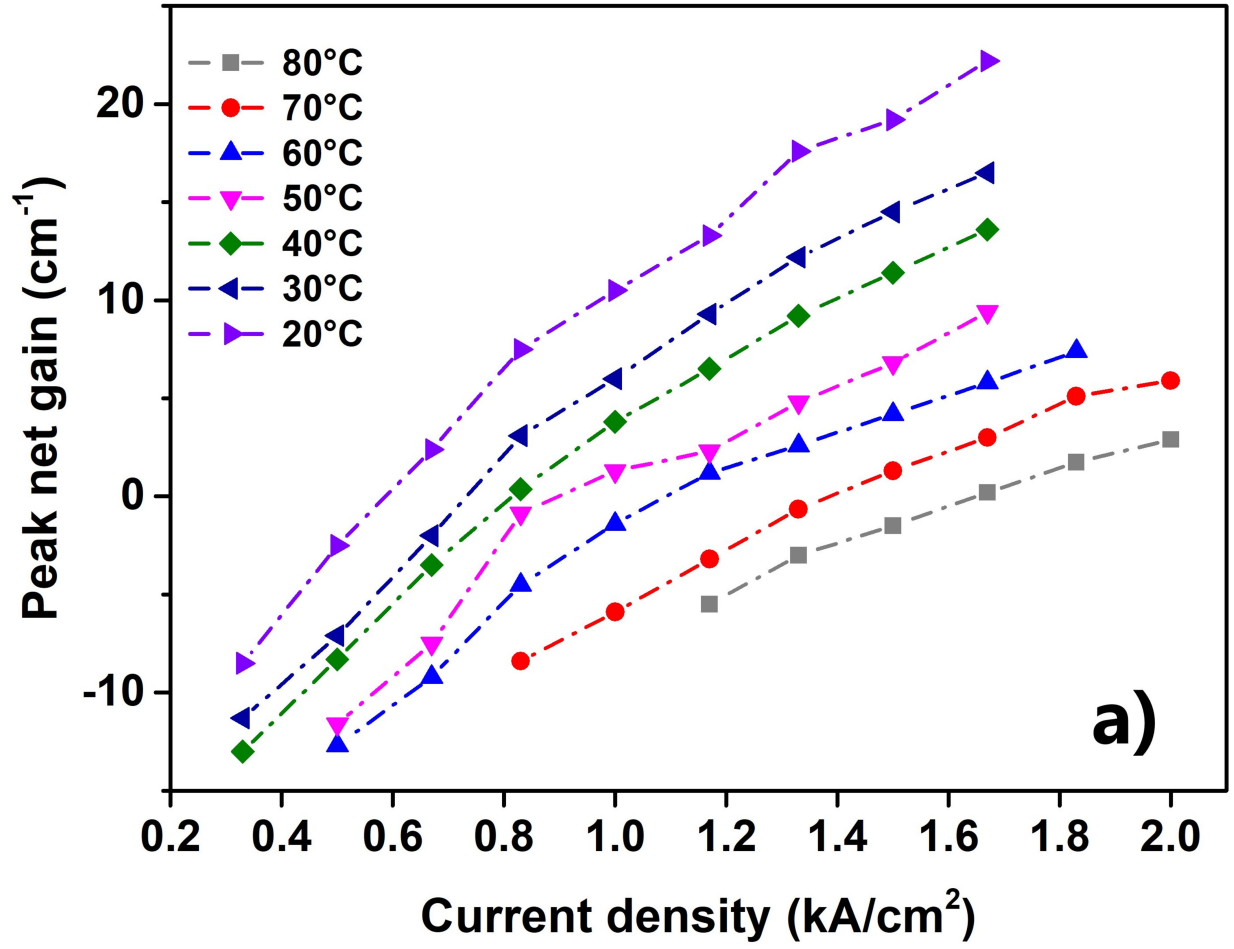
This is the author's peer reviewed, accepted manuscript. However, the online version of record will be different from this version once it has been copyedited and typeset.

PLEASE CITE THIS ARTICLE AS DOI: 10.1063/5.0043815



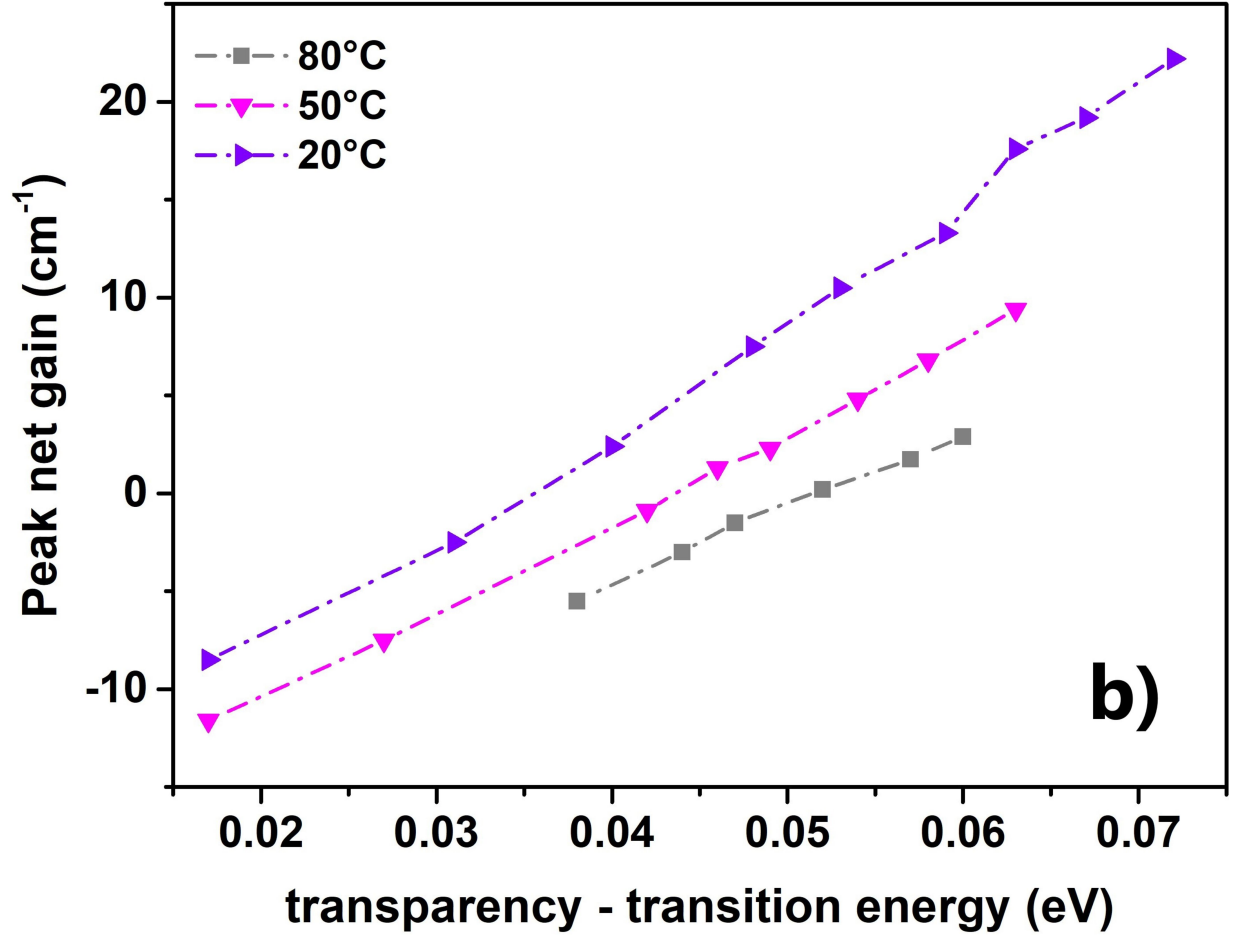
This is the author's peer reviewed, accepted manuscript. However, the online version of record will be different from this version once it has been copyedited and typeset.

PLEASE CITE THIS ARTICLE AS DOI: 10.1063/5.0043815



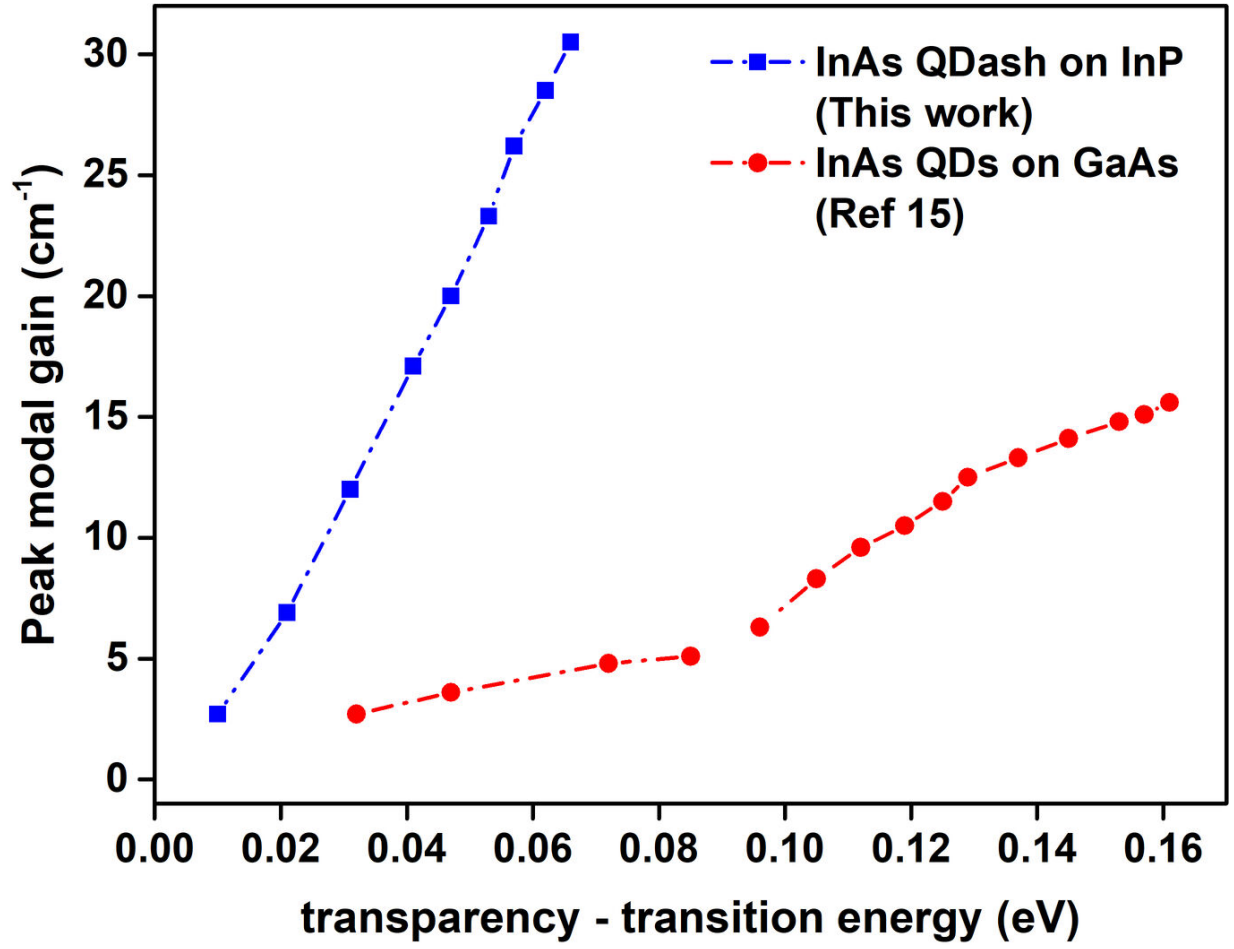
This is the author's peer reviewed, accepted manuscript. However, the online version of record will be different from this version once it has been copyedited and typeset.

PLEASE CITE THIS ARTICLE AS DOI: 10.1063/5.0043815



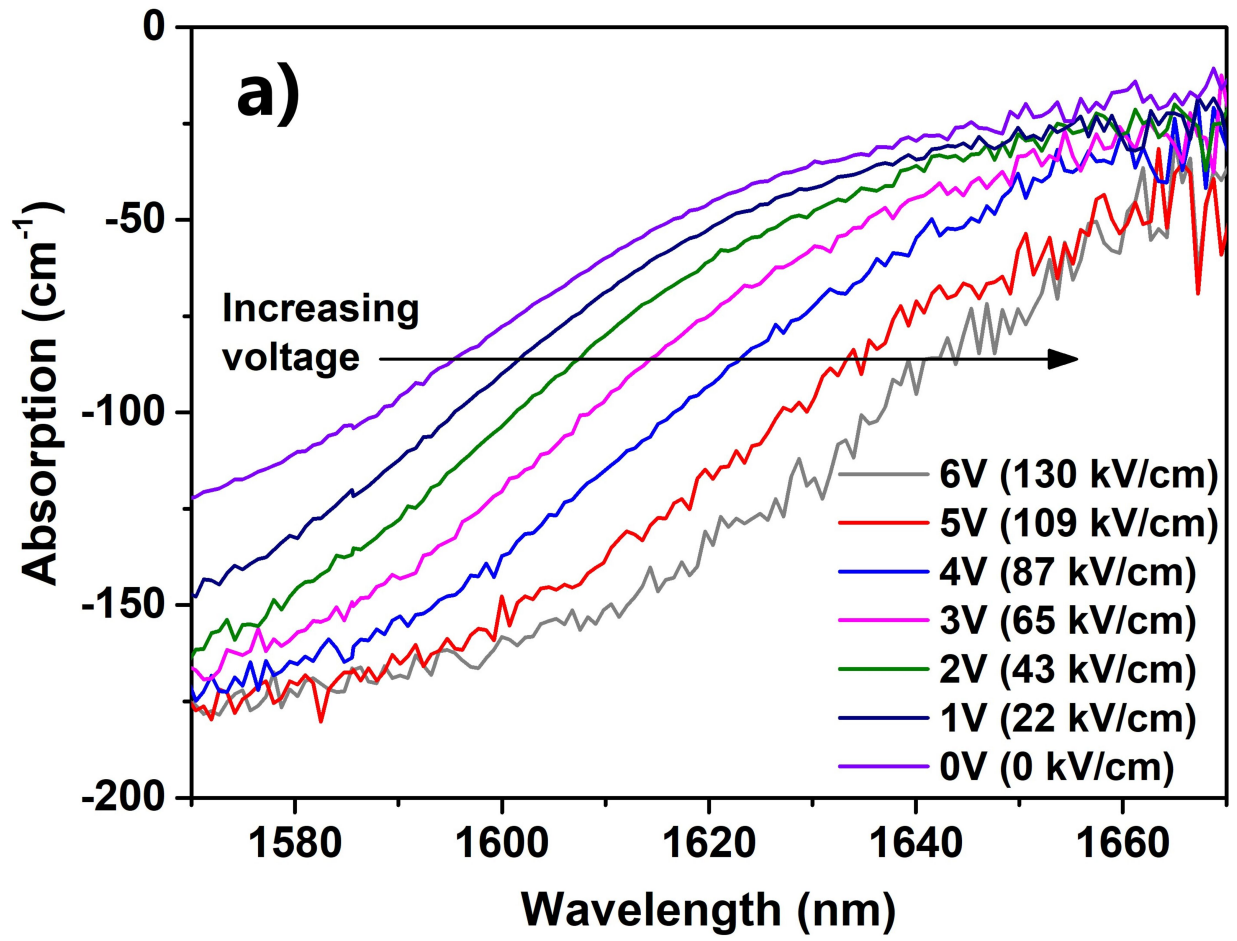
This is the author's peer reviewed, accepted manuscript. However, the online version of record will be different from this version once it has been copyedited and typeset.

PLEASE CITE THIS ARTICLE AS DOI: 10.1063/5.0043815



This is the author's peer reviewed, accepted manuscript. However, the online version of record will be different from this version once it has been copyedited and typeset.

PLEASE CITE THIS ARTICLE AS DOI: 10.1063/5.0043815



This is the author's peer reviewed, accepted manuscript. However, the online version of record will be different from this version once it has been copyedited and typeset.

PLEASE CITE THIS ARTICLE AS DOI: 10.1063/5.0043815

